The thermal-transport properties of the $Ca_{3-x}Ag_xCo_4O_9$ system ($0 \leq x \leq 0.3$)

2007 J. Phys.: Condens. Matter 19 356216

(http://iopscience.iop.org/0953-8984/19/35/356216)

J. Phys.: Condens. Matter **19** (2007) 356216 (10pp) doi:10.1088/0953-8984/19/35/356216

The thermal-transport properties of the $Ca_{3-x}Ag_xCo_4O_9$ system ($0 \leqslant x \leqslant 0.3$)

Yang Wang[1], Yu Sui[1,2,3], Jinguang Cheng[1], Xianjie Wang[1] and Wenhui Su[1,2]

[1] Center for Condensed Matter Science and Technology (CCMST), Department of Physics, Harbin Institute of Technology, Harbin 150001, People's Republic of China
[2] International Centre for Materials Physics, Chinese Academy of Sciences, Shenyang 110016, People's Republic of China

E-mail: suiyu@hit.edu.cn

Received 15 March 2007, in final form 10 June 2007
Published 20 August 2007
Online at stacks.iop.org/JPhysCM/19/356216

Abstract

Polycrystalline $Ca_{3-x}Ag_xCo_4O_9$ ($0 \leqslant x \leqslant 0.3$) samples were prepared by solid-state reaction and their thermo-transport properties were studied from 5 K to room temperature. With the substitution of Ag^+ for Ca^{2+}, the internal chemical pressure induced by Ag^+ doping has a strong effect on the transport properties of such a strongly correlated Fermi liquid system. The electrical conductivity and the thermoelectric power increase simultaneously because of the enhancement of carrier concentration and the change of carrier mobility. The thermal conductivity decreases monotonically up to $x = 0.3$ due to the Ag ion acting as a rattler in the system. These results showed that the thermoelectric performance of the $Ca_3Co_4O_9$ system can be improved by doping with Ag.

1. Introduction

As a kind of promising energy-conversion material in harmony with our environment, thermoelectric materials have attracted a renewed interest. Among them, the layered cobalt oxides have been investigated extensively in recent years due to the discovery of large thermoelectric power (S) coexisting with low resistivity (ρ) and low thermal conductivity (κ) in $NaCo_2O_4$ [1]. In this family, the misfit-layered $Ca_3Co_4O_9$ system, which also shows high thermoelectric performance, is more favoured for practical application because of its thermal and chemical stability at high temperature [2–8]. It has been predicted theoretically that the average valence of cobalt can play an important role in the thermoelectric properties of cobalt oxides [9]. So adjusting the average valence of cobalt and thus the carrier concentration by substitution is a feasible route for enhancing the thermoelectric performance [10, 11].

A large thermoelectric figure of merit ($ZT = S^2T/\rho\kappa$) is necessary for practical thermoelectric materials, which requires a large S but a small ρ and κ. However, these three

[3] Author to whom any correspondence should be addressed.

parameters are all functions of carrier concentration and are interrelated with each other. For most materials, S and ρ are both in inverse proportion to the carrier concentration, so usually an increase of S induced by doping also results in an increase of ρ. For instance, the substitution with a trivalent cation (such as rare-earth ions) for Ca^{2+} in the $Ca_3Co_4O_9$ system can increase S together with ρ due to the decrease of the number of hole charge-carriers while the substitution with univalent cation will show an opposite result [11, 12]. However, it has been discovered that substitution with univalent Na^+ for Ca^{2+} can reduce ρ but enhance S simultaneously, resulting in the remarkable enhancement of the power factor $P(=S^2/\rho)$ [8, 10]. The physical nature of such anomalous behaviour is still controversial, but it is commonly considered that the strong correlations between electrons play an important role [8, 22]. Moreover, the thermal conductivity κ, including lattice thermal conductivity and carrier thermal conductivity, is more dependent on the lattice vibration rather than carrier concentration because lattice thermal conductivity is dominant in a $Ca_3Co_4O_9$ system. Therefore, doping with heavy ions can suppress the lattice contribution to κ. In this case, as a light element, the substitution of Na^+ leads to the increase of κ, and thus it is unfavourable for the increase of the ZT value. As an alternative choice, the doping of univalent Ag^+, which is much heavier than Ca^{2+}, may reduce κ but keep decreasing ρ and enhancing S, so the thermoelectric performance can evidently be improved. In addition, a detailed study of the transport properties of the doped $Ca_3Co_4O_9$ system is useful for clarifying the nature of its high thermoelectric performance.

In this paper, the transport and thermoelectric properties of polycrystalline $Ca_{3-x}Ag_xCo_4O_9$ ($0 \leqslant x \leqslant 0.3$) samples were systematically investigated from 5 K to room temperature. We found that the Ag ion can have a strong effect on the electric and thermal transport properties of the system, and the thermoelectric performance of the $Ca_3Co_4O_9$ system can be improved by the substitution of Ag for Ca.

2. Experiment

The $Ca_{3-x}Ag_xCo_4O_9$ polycrystalline samples ($x = 0$, 0.05, 0.1, 0.15 and 0.3) were prepared by a solid-state reaction method. Reagent-grade $CaCO_3$, Co_2O_3 and $AgNO_3$ powders in the stoichiometric ratio were mixed thoroughly and calcined in air at 1173 K for 12 h. Then the mixture was reground, pressed into a disc-shaped pellet and sintered at 1223 K for 36 h under an O_2 flow with an intermediate grinding. X-ray diffraction (XRD) data at room temperature were collected using a Bede D^1 x-ray diffractometer with Ni-filtered Cu Kα ($\lambda = 0.154\,06$ nm) radiation. The temperature dependences of resistivity, thermoelectric power and thermal conductivity were performed by using a standard four-probe method. The thermoelectric power was calculated according to $S = \Delta V/\Delta T$ by measuring the thermoelectric voltage (ΔV) and the temperature gradient (ΔT) across the sample. The thermal conductivity was measured using a steady-state technique in a closed refrigerator pumped down to 10^{-5} Torr. The Hall effect measurements were performed by a five-probe method. The Hall resistivity under magnetic field was measured in different temperatures, and then the Hall coefficient and the carrier concentration of the samples were obtained. All the measurements above were carried out by using a commercial Quantum Design physical property measurement system (PPMS-9T). The typical dimensions of the measured sample are $10 \times 1.5 \times 1.0$ mm^3.

3. Results and discussion

Figure 1 shows the x-ray powder diffraction patterns for the $Ca_{3-x}Ag_xCo_4O_9$ ($x = 0$, 0.1 and 0.3) ceramics, which are identical to the standard JCPDS card (21-139) of $Ca_9Co_{12}O_{28}$, indicating the formation of single-phase compounds at room temperature. Other samples have the same XRD patterns as the above specimens. These results indicate that Ag was doped

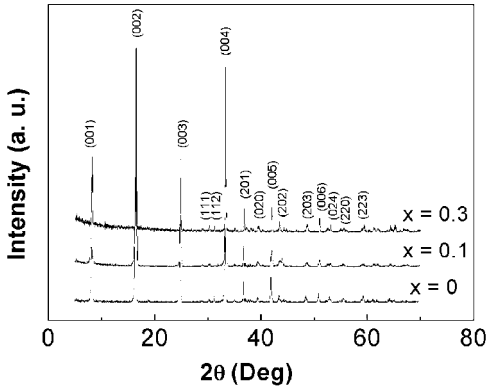

Figure 1. XRD patterns for the $Ca_{3-x}Ag_xCo_4O_9$ ($x = 0$, 0.1 and 0.3) ceramics.

Table 1. Lattice parameters a, b_1, c, and unit-cell volume of $Ca_{3-x}Ag_xCo_4O_9$ polycrystalline samples. Here b_1 is the b-axis length of the rock salt-type Ca_2CoO_3 subsystem [2].

Samples	a (nm)	b_1 (nm)	c (nm)	Unit-cell volume (nm^3)
$Ca_3Co_4O_9$	0.4840(7)	0.4576(1)	1.082(4)	0.23976
$Ca_{2.95}Ag_{0.05}Co_4O_9$	0.4837(2)	0.4572(2)	1.084(8)	0.23992
$Ca_{2.9}Ag_{0.1}Co_4O_9$	0.4833(1)	0.4566(5)	1.088(1)	0.24014
$Ca_{2.85}Ag_{0.15}Co_4O_9$	0.4827(3)	0.4553(2)	1.092(5)	0.24036
$Ca_{2.7}Ag_{0.3}Co_4O_9$	0.4816(3)	0.4535(9)	1.099(7)	0.24123

into the lattice of $Ca_3Co_4O_9$ without any detectable change in the crystal structure. The lattice parameters determined by the Reiveld refinement method, using the profile analysis program FullProf, are shown in table 1. It can be found from table 1 that the lattice parameters a and b_1 decrease simultaneously but c increases strikingly with increasing doping content, meaning a large crystallographic distortion caused by the Ag^+ substitution for Ca^{2+} in $Ca_3Co_4O_9$ lattice.

The variation of the unit-cell parameters gave us clear evidence that, though some doped Ag atoms may diffuse into the interstitial sites rather than Ca sites, the substitution Ag^+ for Ca^{2+} in $Ca_3Co_4O_9$ should be dominant in this system. For one thing, if one compares the ionic radius of Ag^+ and Ca^{2+} (1.15 Å and 1.00 Å respectively in six-coordination), as well as their different valence state, it is inevitable that a distorted bond structure and thus a change in the unit-cell parameters occurs [13]. For another, it is also important to consider the charge distribution in the $Ca_3Co_4O_9$ system. The number of hole carriers will increase with Ag^+ doping according to the valency equilibrium in this system, which leads to an increase in the net positive hole charge distribution in the CoO_2 sublattice. Therefore, due to the layered structure of the system, the repulsion out of the layers increases, and this may cause expansion of the distance between layers, resulting in the obvious increase of lattice parameter c and the unit-cell volume.

Figure 2 shows the temperature dependence of resistivity (ρ) of $Ca_{3-x}Ag_xCo_4O_9$ from 5 to 300 K. All the samples show similar transport behaviour, and the resistivity decreases with increasing Ag content. The decrease of ρ can be attributed to the substitution of univalent Ag^+ for divalent Ca^{2+} in this compound. The carrier of the $Ca_3Co_4O_9$ system is the hole, coming from the CoO_2 sublattice [2]. The hopping of holes between Co^{3+} and Co^{4+} is responsible for the electric conductivity. Based on the valency equilibrium, the substitution of Ag^+ for Ca^{2+} in $Ca_3Co_4O_9$ will create more hole carriers, and consequently decrease the resistivity. This result is consistent with the Hall effect measurement. From the Hall coefficient R_h and the carrier

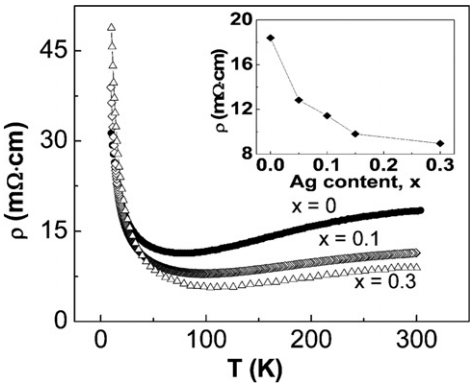

Figure 2. Temperature dependence of resistivity of $Ca_{3-x}Ag_xCo_4O_9$ for $x = 0$, 0.1 and 0.3 from 5 to 300 K; the inset shows the Ag content dependence of ρ at 300 K.

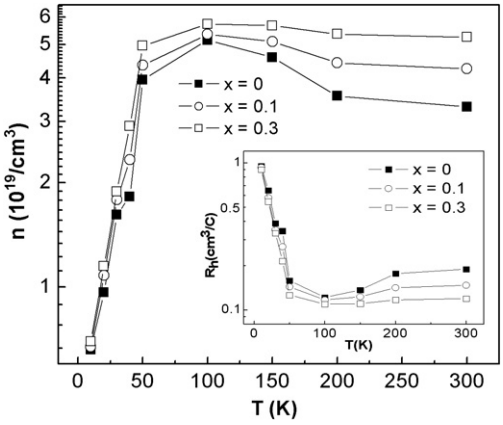

Figure 3. The carrier concentration n of $Ca_{3-x}Ag_xCo_4O_9$ for $x = 0$, 0.1 and 0.3 at different temperatures; the inset shows the corresponding Hall coefficient R_h.

concentration n shown in figure 3, the positive Hall coefficient for all the samples implies that the charge carriers are hole-like in this system. It can be found that n increases with the increase of the doping level in the whole temperature range, so the resistivity decreases as a result. We can also make an estimation about the increase of the hole concentration with x. Assuming there is only one hole carrier per $Ca_3Co_4O_9$ molecule, when the Ag doping content is equal to x (x ranges from 0 to 0.3), it can introduce an additional hole and then the amount of hole will be $(1 + x)$ per $Ca_3Co_4O_9$ molecule, so the hole concentration will increase $(x \times 100)$ per cent, compared with undoped $Ca_3Co_4O_9$. This result roughly accords with the Hall measurement. For example, when $x = 0.1$ and 0.3, we estimate that the increases of hole concentration are 0.34×10^{19} cm^{-3} and 1.01×10^{19} cm^{-3} at 300 K, while Hall measurements show that the increases of the hole concentration are 0.95×10^{19} cm^{-3} and 1.93×10^{19} cm^3 at 300 K respectively. Moreover, the Hall coefficient R_h exhibits obvious temperature dependence, consistent with the characteristic of a strongly correlated system [14].

The temperature dependence of ρ for the $Ca_3Co_4O_9$ system shows two characteristic temperatures between 5 and 300 K, T_{M-I} and T^*. The $Ca_3Co_4O_9$ system is a strongly correlated Fermi liquid in the temperature range between T_{M-I} and T^*, with a resistivity variation of $\rho = \rho_0 + AT^2$, where A is the Fermi liquid transport coefficient [15]. All $Ca_{3-x}Ag_xCo_4O_9$ samples exhibit such a temperature region as shown in the inset of figure 4, where T_{M-I} and T^* are defined as the onset and end temperature of the linear dependence for $\rho \sim T^2$. T_{M-I} corresponds to the metal-to-insulator transition temperature around 80 K and T^* is usually interpreted as the transition temperature from Fermi liquid to incoherent

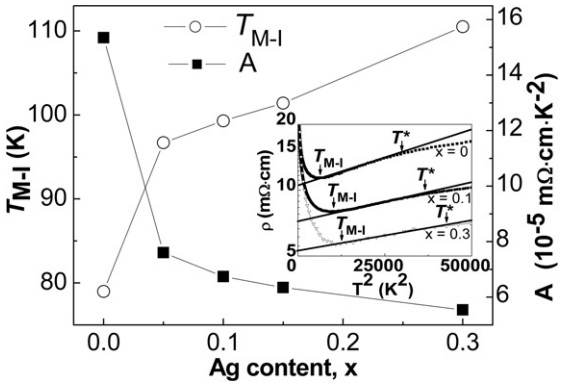

Figure 4. Ag content dependence of T_{M-I} and the Fermi liquid transport coefficient A; the inset shows ρ versus T^2 with the fitted lines, and the plots of ρ versus T^2 for all the samples lie on straight lines between T_{M-I} and T^*.

metal around 150 K [15, 16]. With increasing Ag concentration, the transition temperatures (both T_{M-I} and T^*) increase and the slope A decreases simultaneously, as shown in figure 4. The increase of T_{M-I} (or T^*) and the decrease of A under hydrostatic pressure had been observed in the $Ca_3Co_4O_9$ sample, which is the typical behaviour of strongly correlated Fermi liquid [15, 16]. In the $Ca_{3-x}Ag_xCo_4O_9$ system, the large difference between the ionic radii of Ag^+ and Ca^{2+}, which are 1.15 Å and 1.00 Å respectively in six-fold coordination, as well as the crystallographic distortion will cause notable chemical pressure inside the lattice that will be enhanced with the increase of the doping level. Therefore, in the Ag^+-doped $Ca_3Co_4O_9$ system, this chemical pressure can serve the same effect as hydrostatic pressure in the $Ca_3Co_4O_9$ system, and thus affect the transport properties in such a strongly correlated Fermi liquid.

For all the samples there is an M–I transition in the temperature range 80–110 K. The M–I transition around 80 K of $Ca_3Co_4O_9$ is considered to be correlated to the existence of an incommensurate spin-density-wave (IC-SDW) [17, 18]. It has been reported that from high temperature (about 600 K) to low temperature (about 19 K), the $Ca_3Co_4O_9$ system changes from a paramagnetic semiconducting state to a paramagnetic metallic state (∼380 K) and to an IC-SDW insulating state (∼100 K), and then to a ferrimagnetic insulating state (∼19 K) [17–19]. Just the appearance of the IC-SDW localizes the charge carrier and results in the insulating behaviour of the system below T_{M-I} [17]. Therefore the onset temperature of the IC-SDW transition T_{SDW}^{ON} (∼100 K) is consistent with the M–I transition temperature T_{M-I} (∼80 K), where a broad minimum around T_{M-I} in the $\rho(T)$ curve can been seen. The IC-SDW transition depends on the average valence of the Co ions, because it is found that Sr^{2+} substitution for Ca^{2+} in the $Ca_3Co_4O_9$ system has no significant effect on the IC-SDW, and Y^{3+} or Bi^{3+} doping increased T_{SDW}^{ON} owing to the reduction of the average valence of Co ions [17–19]. Therefore the univalent Ag^+ doping should decrease T_{SDW}^{ON} and thus result in decreasing the T_{M-I}. But the decrease of T_{M-I} due to valence variation may be overcome by the increase of T_{M-I} caused by the large chemical pressure, and then lead to the increase of T_{M-I} finally in $Ca_{3-x}Ag_xCo_4O_9$ samples.

Figure 5 shows the temperature dependence of the thermoelectric power (S) of $Ca_{3-x}Ag_xCo_4O_9$ in the range from 5 to 300 K. The positive S for all the samples indicates their hole conduction nature, and the increase of S with increasing the doping level is similar to the results found in the Na-substituted $Ca_3Co_4O_9$ system and Ag-substituted $NaCo_2O_4$ system [10, 22]. S can be expressed by the formula

$$S(T) = \frac{1}{eT}\frac{\int_{-\infty}^{\infty}\sigma(\varepsilon)(\varepsilon-\mu)\frac{\partial f(\varepsilon)}{\partial\varepsilon}\,\mathrm{d}\varepsilon}{\int_{-\infty}^{\infty}\sigma(\varepsilon)\frac{\partial f(\varepsilon)}{\partial\varepsilon}\,\mathrm{d}\varepsilon}, \tag{1}$$

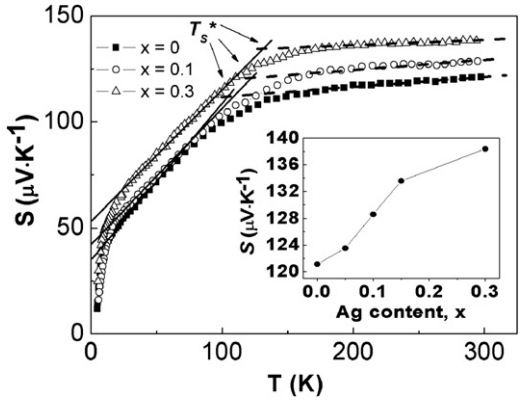

Figure 5. Temperature dependence of thermoelectric power of $Ca_{3-x}Ag_xCo_4O_9$ for $x = 0, 0.1$ and 0.3 from 5 to 300 K; the solid lines are the fitting data by using $S(T) = S^*(T) + S_0$ below $T^*/2$ and the dashed lines are the fitting straight lines for S above T^*. T_S^* is defined as the crossing point of the solid line and dashed line for each sample. The inset shows the Ag content dependence of S at 300 K.

where $\sigma(\varepsilon)$ and $f(\varepsilon)$ represent the electrical conductivity and Fermi–Dirac distribution function at the energy ε [20, 21]. By using the condition of $\partial f(\varepsilon)/\partial\varepsilon = \delta(\varepsilon = \varepsilon_F)$ and $\sigma = en\mu(\varepsilon)$ [21, 23], formula (1) can turn into

$$S(T) = \frac{c_e}{n} + \frac{\pi^2 k_B^2 T}{3e}\left[\frac{\partial \ln \mu(\varepsilon)}{\partial \varepsilon}\right]_{\varepsilon=\varepsilon_F}, \tag{2}$$

where n, $\mu(\varepsilon)$, c_e, k_B, $\psi(\varepsilon)$ are carrier concentration, energy correlated carrier mobility, specific heat, Boltzmann constant and density of state, respectively. Formula (2) consists of two terms, but the first term c_e/n is the inverse of the carrier concentration. So the second term of (2) should be dominant in describing the S of the $Ca_{3-x}Ag_xCo_4O_9$ samples because the value of S increases with the increase of carrier concentration. Therefore, it can be concluded that $\mu(\varepsilon)$ may play a crucial role in determining the thermoelectric power in such layered cobalt oxides, and just the change of $\mu(\varepsilon)$ with doping Ag results in the increase of S, which is similar to what is found in the Na-substituted $Ca_3Co_4O_9$ system [8, 10].

Such behaviour can also be understood by considering the valence states of Ag^+ and Ca^{2+}. Ag^+ substitution for Ca^{2+} in the crystal lattice will change the Fermi level E_F and valence band energy E_V of the system, i.e. the band structure that depends on the nominal valence state of Co ions, Co^{n+}. According to the band calculation of misfit-layered cobalt oxide containing a CoO_2 sheet [24, 25], the density of states (DOS) near E_F consists of the localized band and the itinerant band; the height of E_F depends on $n+$. Due to the valency equilibrium for Ag^+ substitution, the parameter $n+$ gradually increases towards Co^{4+}, and E_F as well as E_V will change. In the case of a band semiconductor in which the relation time τ is described by

$$\tau = \tau_0 E^{r-1/2} \tag{3}$$

where E is the relaxation energy of carriers and r is the scattering parameter, the thermoelectric power S takes the form

$$S \sim \frac{k_B r}{e} + \frac{E_F - E_V}{eT}. \tag{4}$$

Therefore we propose that Ag^+ substitution for Ca^{2+} induces more enhancement of E_F than E_V, arising from changes in the band structure, and then results in the increase of S.

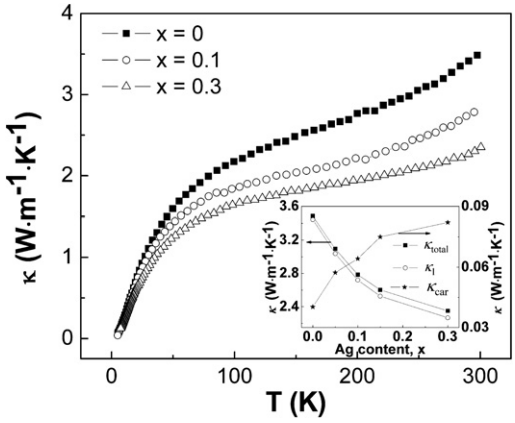

Figure 6. Temperature dependence of the thermal conductivity of $Ca_{3-x}Ag_xCo_4O_9$ for $x = 0$, 0.1 and 0.3 from 5 to 300 K; the inset shows the Ag content dependence of total thermal conductivity κ_{total}, lattice thermal conductivity κ_l and carrier thermal conductivity κ_{car} at 300 K.

For all the samples, figure 5 also displays that the temperature dependence of S from about 20 K up to $T^*/2$ can be described using a renormalized free-electron thermoelectric power S^* theory [15, 26],

$$S(T) = S^*(T) + S_0 = \left(\frac{\pi^2}{6}\right)\frac{k_B T}{eT^*} + S_0, \tag{5}$$

where S_0 is the constant thermoelectric power and T^* is the transition temperature mentioned above. Due to the proportionality between S^* and the inverse of T^*, the slope of $S(T)$ will decrease with doping because of the increase of T^* under chemical pressure. The fitting solid lines in figure 5 show that the slope of $S(T)$ decreases from 0.74 to 0.61 μV K^{-2} while the doping level increases from $x = 0$ to 0.3. If we define T_S^* as the crossing point of the solid line and the dashed line shown in the figure, the change of T_S^* by doping is also consistent with T^*. However, the physical meaning of T_S^* together with the relationship among T_S^*, T^* and T_{M-I} calls for further studies. The origin of S_0 is not clear, but the increase of S_0 with doping suggests that the contribution from defects or impurities may be a possible candidate for S_0. Although S_0 increases with doping, we must emphasize that the major contribution still comes from renormalized carriers giving rise to S as $S(T) = S^*(T) + S_0$ below T_S^*. Moreover, S at low temperature can also agree with $S(T) \sim (\gamma/C)T + S_0$ [26], where γ is the electric specific heat coefficient and C is a parameter. The reduction of γ due to the decrease of slope with doping suggests a decrease of electronic correlations by Ag^+ substitution in the system, which is another typical behaviour of a strongly correlated system under pressure. As for the deviation from linearity for S below 20 K, the absence of the spin degree of freedom of the Co ion caused by magnetic order may be responsible [17]. The appearance of a ferrimagnetic order could evidently reduce the entropy of the system and then induce a drop of S below 20 K.

Figure 6 displays the temperature dependence of the thermal conductivity (κ) of $Ca_{3-x}Ag_xCo_4O_9$. All the samples show similar thermal transport behaviour, but κ decreases monotonically with an increasing Ag^+ content. At room temperature, the κ value decreases from about 3.5 W m^{-1} K^{-1} for $Ca_3Co_4O_9$ to about 2.2 W m^{-1} K^{-1} for the $x = 0.3$ sample. The thermal conductivity κ can be expressed by the sum of the lattice component (κ_l) and the carrier component (κ_{car}) as $\kappa = \kappa_l + \kappa_{car}$. The κ_{car} values can be calculated from Wiedemann–Franz's law as $\kappa_{car} = L_0 T/\rho$, where $L_0 = \pi^2 k_B^2/3e^2$ is the Lorentz constant. As shown in the inset of figure 6, the contribution of κ_{car} to thermal conductivity is quite small for all the samples (less than 5%), so κ_l is the predominant component in the thermal conductivity of $Ca_{3-x}Ag_xCo_4O_9$. Therefore the reduction in κ mainly originates from the change of κ_l on doping Ag.

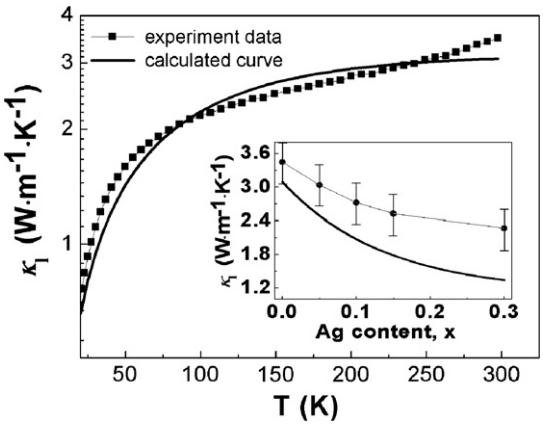

Figure 7. Temperature dependence of the lattice thermal conductivity (κ_l) of $Ca_3Co_4O_9$; the curve is the calculation for $Ca_3Co_4O_9$ by the theory of Callaway [27, 28]; the inset shows the variation of the lattice thermal conductivity of $Ca_{3-x}Ag_xCo_4O_9$ at 300 K, and the curve is the behaviour calculated according to [28].

According to the phonon-scattering theory of Callaway [27, 28], the total scattering rate τ^{-1} is given as

$$\tau^{-1} = \tau_{pd}^{-1} + \tau_{ph-ph}^{-1} + \tau_0^{-1} = A\omega^4 + B\omega^2 + v/L, \tag{6}$$

where τ_{pd}^{-1}, τ_{ph-ph}^{-1} and τ_0^{-1} are the scattering rates for point-defect scattering, phonon–phonon scattering and boundary scattering. These three scattering rates equal $A\varpi^4$, $B\varpi^2$ and v/L respectively, where ω, v are the phonon frequency and mean sound velocity, and A, B, L are characteristic parameters. The phonon–phonon scattering usually gives $\kappa \propto 1/\sqrt{AT}$ [28], but κ for $Ca_{3-x}Ag_xCo_4O_9$ increases with T, indicating that the phonon–phonon scattering τ_{ph-ph}^{-1} is negligible, just as reported in the Ca-doped $NaCo_2O_4$ system [29]. So the point-defect scattering τ_{pd}^{-1} plays an important role in the change of the total scattering rate τ^{-1} because the boundary scattering τ_0^{-1} should remain invariable after doping due to the same synthesis conditions of these samples. A can be expressed as [31]

$$A = \Omega_0 \sum f_i (1 - M_i/M_{av})^2/4\pi v^3, \tag{7}$$

where Ω_0 is the unit-cell volume, M_i is the mass of each atom, f_i is the fraction of an atom with mass, and $M_{av} = \sum f_i M_i$ is the average mass. By the method of Meisner *et al* [32], in the case of only doping one kind of atom with relative concentration α, formula (7) will change into

$$A = \frac{1}{4\pi v^3}\left[\Omega_0 \alpha (1-\alpha)(\Delta M/M_{av})^2\right], \tag{8}$$

where ΔM is the difference between the mass of the doped atom and that of the host. The value of A for $Ca_{3-x}Ag_xCo_4O_9$ calculated by formula (8) increases from 1.1×10^{-40} to 4.5×10^{-40} s^3 on increasing the doping level from $x = 0.05$ to $x = 0.3$. So the total scattering rate τ^{-1} will increase with Ag doping, and then κ_l will decrease consequently. The mean sound velocity $v = 4022$ m s^{-1} at 300 K can be determined according to $\theta = (\hbar v/k_B)(6\pi^2 N)^{1/3}$ by using the Debye temperature $\theta = 660$ K obtained from the specific heat data of $Ca_3Co_4O_9$ [30]. It can be seen from figure 7 that, according to the theory of Callaway and von Baeyer [28, 31], the calculated curve of the lattice thermal conductivity of $Ca_3Co_4O_9$ is consistent with experimental data. This result confirms that the point-defect scattering mechanism is dominant in determining the thermal conductivity of this system, and the results can account well for the decrease in thermal conductivity with doping of the Ag ions, as shown in the inset of figure 7.

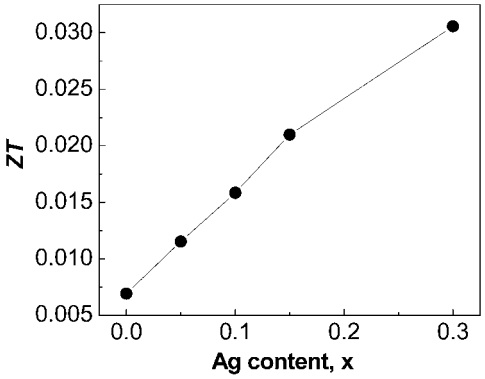

Figure 8. Ag content dependence of the figure of merit ZT of $Ca_{3-x}Ag_xCo_4O_9$ at 300 K.

Actually, the substitution of Ag^+ for Ca^{2+} can affect the lattice vibration of the system strongly. The effect of Ag doping on lattice vibration originates from two main aspects. One is the crystallographic distortion caused by the difference between the Ag^+ and Ca^{2+} ionic radii. The other, more important to thermal transport, is that the weight of Ag^+ is much heavier than Ca^{2+}. Because of the large difference between the weight of Ag^+ and Ca^{2+}, Ag ions can act as rattlers bounded in 'atom cages', so they will vibrate independently from the other atoms and cause large local vibration. As a result, the phonon mean free path will be shortened, and then κ_l will decrease. At the same time, with an increasing doping level, the enhanced scattering of lattice defect and impurity increase will also shorten the mean free path of the phonon and result in the decrease of κ_l. Therefore the total thermal conductivity κ can be anticipated to decrease with an increasing doping level. In addition, we make a rough estimate of the phonon mean free path (l_{ph}) for the $x = 0.3$ sample according to $\kappa_l = Cvl_{ph}/3$, where C is the lattice specific heat, and get $l_{ph} = 1.03$ nm at 300 K. The value of l_{ph} is comparable with the lattice parameter and much shorter than the electron mean free path (∼10 nm), suggesting that the Ag-doped $Ca_3Co_4O_9$ system can act as a kind of 'phonon glass and electron crystal' material, which is usually considered as an ideal candidate for a practical thermoelectric device.

The change of ρ, S and κ with the doping level indicates that the thermoelectric performance of $Ca_3Co_4O_9$ system can be improved effectively by Ag substitution. As shown in the figure 8, the value of the figure of merit $ZT(=S^2T/\rho\kappa)$ of $Ca_{3-x}Ag_xCo_4O_9$ increases with increasing the Ag content, and the ZT value of the $x = 0.3$ sample reaches 0.03 at room temperature, which is about five times larger than that of the undoped sample.

4. Conclusions

Ag was successfully doped at the Ca site by up to 10% in the $Ca_3Co_4O_9$ ceramic by a solid-state reaction method without changing the crystal structure. Investigation of the transport and thermoelectric properties of the $Ca_{3-x}Ag_xCo_4O_9$ system has revealed the following.

(1) The substitution of Ag^+ for Ca^{2+} provides a significant decrease of ρ and an increase of S simultaneously due to the enhancement of the carrier concentration and the change of the carrier mobility.
(2) The chemical pressure inside the system induced by Ag^+ doping has a strong effect on the transport properties, and it shows that such chemical pressure has the same effect as hydrostatic pressure in the $Ca_3Co_4O_9$ strongly correlated Fermi liquid.
(3) At low temperature, S can be described by a renormalized free-electron thermoelectric power theory, and the characteristic temperature T_S^* increases with doping, which is consistent with T_{M-I} and T^*.

(4) The point-defect scattering is dominant in describing the thermal transport of the system, and the substitution of Ag^{+} is favourable for the reduction of κ, because the Ag ion can act as a rattler. In this way, the Ag-doped $Ca_3Co_4O_9$ system seems to be a material which is a phonon glass and an electron crystal.
(5) With an increasing Ag doping level, the ZT value can be enhanced and reaches 0.03 at 300 K, which is quite large for oxides. This means that such a heavy ion doped strongly correlated system with a layered structure may be a potential candidate for a thermoelectric device.

Acknowledgments

This work was supported by the National Natural Science Foundation of China (Grant Nos 10304004 and 50672019).

References

[1] Terasaki I, Sasago Y and Uchinokura K 1997 *Phys. Rev.* B **56** R12685
[2] Masset A, Michel C, Maignan A, Hervieu M, Toulemonde O, Studer F, Reveau B and Hejtmanek J 2000 *Phys. Rev.* B **62** 166
[3] Siwen L, Funahashi R, Matsubara I, Ueno K and Yamada H 1999 *J. Mater. Chem.* **9** 1659
[4] Yuqi Z *et al* 2003 *J. Appl. Phys.* **93** 2653
[5] Funahashi R and Matsubara I 2001 *Appl. Phys. Lett.* **79** 362
[6] Miyazaki Y, Onoda M, Oku T, Kikuchi M, Ishii Y, Ono Y, Morii Y and Kajitani T 2002 *J. Phys. Soc. Japan* **71** 491
[7] Shikano M and Funahashi R 2003 *Appl. Phys. Lett.* **82** 1851
[8] Xu G J, Funahashi R, Shikano M, Matsubara I and Zhou Y Q 2002 *Appl. Phys. Lett.* **80** 3760
[9] Koshibae W, Tsutsui K and Maekawa S 2000 *Phys. Rev.* B **62** 6869
[10] Xu G J, Funahashi R, Shikano M, Pu Q R and Liu B 2002 *Solid State Commun.* **124** 73
[11] Wang D L, Chen L D, Yao Q and Li J G 2004 *Solid State Commun.* **129** 615
[12] Masuda Y, Nagahama D, Itahara H, Tani T, Seo W S and Koumoto K 2003 *J. Mater. Chem.* **13** 1094
[13] Aksan M A and Yakinci M E 2007 *J. Alloys Compounds* **433** 22
[14] Merino J and McKenzie R H 2000 *Phys. Rev.* B **61** 7996
[15] Limelette P, Hardy V, Auban-Senzier P, Jérome D, Flahaut D, Hébert S, Frésard R, Simon C, Noudem J and Maignan A 2005 *Phys. Rev.* B **71** 233108
[16] Limelette P, Wzietek P, Florens S, Georges A, Costi T A, Pasquier C, Jérome D, Mézière C and Batail P 2003 *Phys. Rev. Lett.* **91** 016401
[17] Sugiyama J, Xia C and Tani T 2003 *Phys. Rev.* B **67** 104410
[18] Sugiyama J, Itahara H, Tani T, Brewer J H and Ansaldo E J 2002 *Phys. Rev.* B **66** 134413
[19] Sugiyama J, Brewer J H, Ansaldo E J, Itahara H, Dohmae K, Seno Y, Xia C and Tani T 2003 *Phys. Rev.* B **68** 134423
[20] McIntosh G C and Kaiser A B 1996 *Phys. Rev.* B **54** 12569
[21] Fisher B, Patlagan L, Reisner G M and Knizhnik A 2000 *Phys. Rev.* B **61** 470
[22] Yakabe H, Fujita K and Nakamura K 1998 *17th Int. Conf. on Thermoelectrics* p 551
[23] Kondo T, Takami T, Takahashi H, Ikuta H, Mizutani U and Soda K 2004 *Phys. Rev.* B **69** 125410
[24] Singh D J 2000 *Phys. Rev.* B **61** 13397
[25] Asahi R, Sugiyama J and Tani T 2002 *Phys. Rev.* B **66** 155103
[26] Ashcroft N W and Mermin N D 1976 *Solid State Physics* (Philadelphia, PA: HoltSaunders)
[27] Callaway J 1959 *Phys. Rev.* **113** 1046
[28] Callaway J and von Baeyer H C 1960 *Phys. Rev.* **120** 1149
[29] Takahata K, Iguchi Y, Tanaka D and Itoh T 2000 *Phys. Rev.* B **61** 12551
[30] Cheng J G *et al* unpublished
[31] Klemens P G 1960 *Phys. Rev.* **119** 507
[32] Meisner G P, Morelli D T, Hu S, Yang J and Uher C 1998 *Phys. Rev. Lett.* **80** 3551